Journal of the European Ceramic Society **18** (1998) 1835–1843

PII: S0955-2219(98)00123-X
0955-2219/98/$—see front matter

Microstructure and Creep of 2·5D C_f–SiC Composites

G. Boitier, J. Vicens and J. L. Chermant*

LERMAT, URA CNRS 1317, ISMRA, 6 bd du Mal Juin, 14050 Caen Cedex, France

Abstract

Tensile creep tests have been performed on 2·5D C_f–SiC composites in parallel to a microstructural characterisation down to the nanometric scale. These ceramic matrix composites (CMCs) appear to be creep resistant when tested under argon (50 mbar), between 1273 and 1673 K, at 110 and 220 MPa. The nanostructure of the different phases involved in the as-received material has been determined via HREM. Microstructural changes and search for creep mechanism have been achieved by SEM. Different types of cracks have been evidenced, and the major role of the fibre/matrix interphase was demonstrated by HREM on tested samples. © *1998 Elsevier Science Limited. All rights reserved*

1 Introduction

The knowledge of high temperature thermomechanical properties of materials—superalloys, ceramics, ceramic matrix composites, etc.—is required for the design bureau. Not only rupture and statistical characteristics are required, but also life time prediction, obtained from creep and fatigue tests under different loads (tension, compression, bending) and environments. In order to obtain information on such parameters and to understand the evolution of the thermomechanical properties of 2·5D C_f–SiC composites under severe conditions of stress and temperature, creep tests have been performed in our laboratory,[1] as well as fatigue tests by Dalmaz.[2]

In the case of ceramics and ceramic matrix composites (CMCs), only uniaxial tests allow access to their mechanical behaviour and constitutive law in a proper way. But for such brittle and high strength materials, the development of precise and reliable tensile tests requires the integration of the different types of basic technological elements—load frame machine, airtight fence, furnace, grips, thermocouple(s), extensometer(s), etc.—keeping in mind a critical point of view on their own restrictions and limits. Moreover, due to the sensitivity of such devices to numerous external parameters—such as the temperature of the test room, the characteristics of the water for the cooled parts, etc.—a particular attention must be taken to so-called secondary parameters most often ignored.

Previous thermomechanical studies have shown on the one hand the importance of the fibre and the fibre/matrix interphase evolution on the mechanical behaviour of CMCs,[3,4] and on the other hand the occurrence of so-called damage-creep mechanisms in CMC.[5–8] For these reasons, we will fully characterise the complete microstructure of both tested and as-received materials, at different scales using scanning electron microscopy (SEM), and transmission and high resolution electron microscopies (TEM and HREM) to clearly identify the mechanisms responsible for creep in such composites.

2 Material and Experimental Devices

2.1 Material

The material under investigation is a C_f–SiC composite fabricated by chemical vapour infiltration (CVI) of a pure SiC matrix within a 2·5D preform of high strength ex-PAN carbon fibres (SEP, Bordeaux, France). The so-called 2·5D architecture corresponds to a stack of five plain woven clothes with a certain interlocking between them. A pyrocarbon interphase has been deposited on the fibre prior to SiC infiltration. A micrograph of such a material is presented in Fig. 1.

2.2 Tensile creep device

High temperature thermomechanical characteristics published on ceramics and ceramic matrix composites are often very dispersed. That can be due not only to the well-known statistical dispersion of the intrinsic defects in ceramics, but also to the fact that experimenters are not careful enough with some experimental and technical errors which lead to biased results. For example, some published

*To whom correspondence should be addressed.

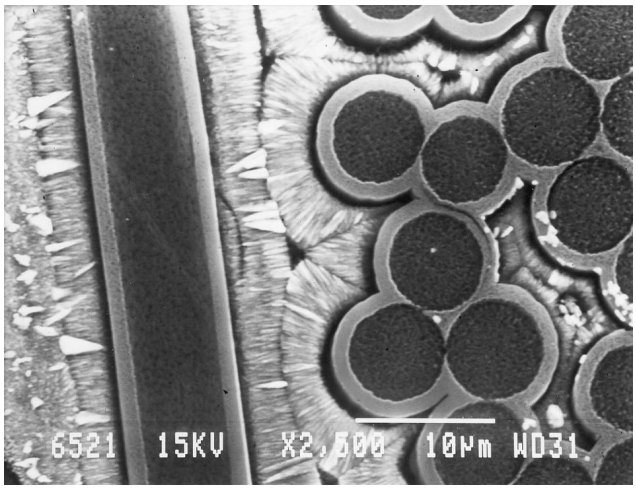

Fig. 1. SEM micrograph of the different phases involved in a 2·5D C_f–SiC composite.

results of life time prediction for silicon nitride can vary over one order of magnitude for measurements performed on exactly the same materials and experimental conditions,[9] which cannot be only attributed to the heterogeneity of the material and/or the presence of defects.

From the experience in our laboratory, we made technological choices in order to develop and optimise a high temperature testing device, based on a critical study of the different possible parts involved.[10,11]

A hydraulic load frame has been chosen to avoid the play of the screws of the columns which is of particular importance when one has to perform loading–unloading cycles to follow the evolution of the elastic modulus of a material. A particular attention has been also paid to the alignment of the frame, and using a tensile instrumented specimen, the percentage of bending (which leads to internal shear stress in the material that can dramatically affect its lifetime) has been reduced to less than 2%.

An induction furnace with a graphite susceptor has been used thanks to its high heating rates and a localised isothermal hot zone on the gauge section of the specimen. An airtight fence was added to the device to allow tests under various environments. Temperature measurement was achieved using a WRh 5/26 thermocouple protected by a tungsten tube to prevent direct reactions with oxygen, carbon or nitrogen which could lead to a significant drift.

Two modified mechanical contact extensometers with SiC arms were used since they are in the same class of precision as laser extensometers, but cheaper and easier to handle.

Tests were conducted in tension under argon partial pressure (50 mbar) for temperatures between 1273 and 1673 K, at stress levels of 110 and 220 MPa.

2.3 Microscopes

A Jeol JSM 6400 SEM was used for damage characterisation. TEM and HREM characterisations were performed to investigate changes in the different phases and the interfacial features at the fibre/matrix interface, using three microscopes operating at 200 kV: a Jeol 200 CX, a Jeol 2010 and a Topcon EM 002B, all equipped with EDX analysis. For such localised investigations, disc-shaped samples ($\varnothing = 3$ mm) were cut from the 2·5D C_f–SiC specimens, then mechanically ground and dimpled to a $\sim$10 µm thickness. The final thinning was achieved by ion-milling (Ar^+, 5 kV).

3 Results

3.1 Microstructural investigation of the as-received 2·5D C_f–SiC composites

The nanostructural study of the as-received composites has been described elsewhere,[12,13] and we will only provide the main results. The β-SiC matrix is columnar, as expected for a CVI processed matrix,[14] with mainly (111) β-SiC planes oriented parallel to the interphase/matrix interface. The pyrocarbon (PyC) interphase texture appears isotropic with a slight orientation of the (0002) planes parallel to the interfaces (i.e. fibre/interphase and interphase/matrix). At both interfaces, the (0002) graphitic planes of the interphase are highly oriented over a few tens of angstroms (Fig. 2) which could suggest fibre/matrix debonding and sliding to occur at the interphase/matrix interface.[15]

Particular attention has been paid to the fibre structure which was shown to be in total agreement with the Guigon's model for high strength ex-PAN carbon fibres.[16] In longitudinal sections, the fibre is composed of tiny and perfect elemental domains, called basic structural units (BSUs), made of 2 to 3 graphitic planes of 0·8–1·0 nm in diameter. The basic structural units rearrange into areas of local molecular orientations (LMOs) which associate to each other along the fibre axis (Fig. 3). The LMOs diameter and thickness measured in the present case are 12·5 and 2·5 nm, respectively. As a result, the (0002) graphitic planes within the longitudinal sections of the fibre have a mean orientation parallel to the fibre axis. In transverse sections, the BSUs are still observed with the same diameter but randomly oriented.

At a larger scale, considering the composite from the bundle point of view, it was shown that the as-received materials are already damaged due to thermal residual stresses developed upon fabrication, as referred by other authors.[2,17,18] Pre-existing cracks are mainly transverse, concentrated

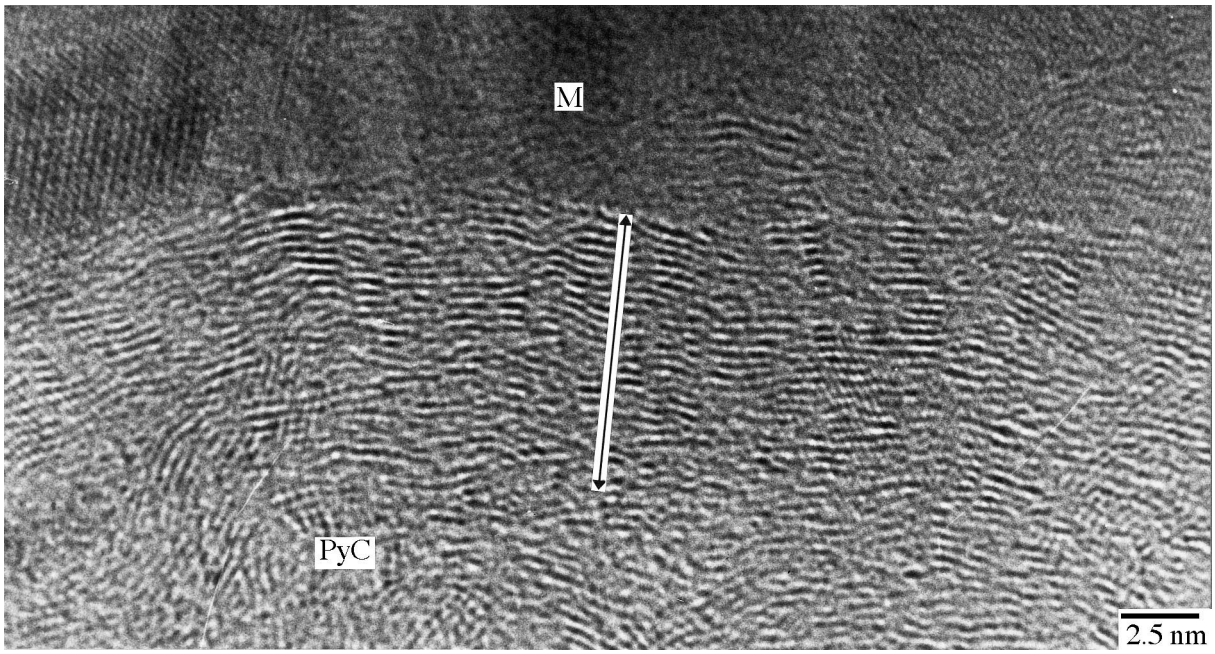

Fig. 2. HREM micrograph of the interphase/matrix (PyC/SiC) interface in an as-received longitudinal section.

within the bundles and perpendicular to the load axis.

3.2 Tensile creep results

As-obtained strain-time creep curves, $\varepsilon = f(t)$, are presented in Fig. 4 (rupture is indicated by vertical arrows). The noise-free shape of the curves underlines the quality of the creep experiments. The shocks observed from time to time are due to unloading-reloading cycles. Each represented curve corresponds to one test, but the scatter is considered close to 10% (some tests were performed on three specimens).

Creep of 2·5D C_f–SiC composites starts at temperature as low as 1273 K, even though it remains small. When rising temperature, the creep strain increases for a given stress level, while, for a given temperature, the creep strain rises with increasing stress.

At 1473 K, under 220 MPa, strain and time to rupture are much lower than at 1673 K, under the same conditions of stress. At 1473 K, the rupture takes place after 82 h for a strain of 1·2%. At 1673 K, the time and strain to failure are 128 h and 2·4%, respectively. This leads to the assumption that a creep mechanism at 1673 K is no more efficient at 1473 K.

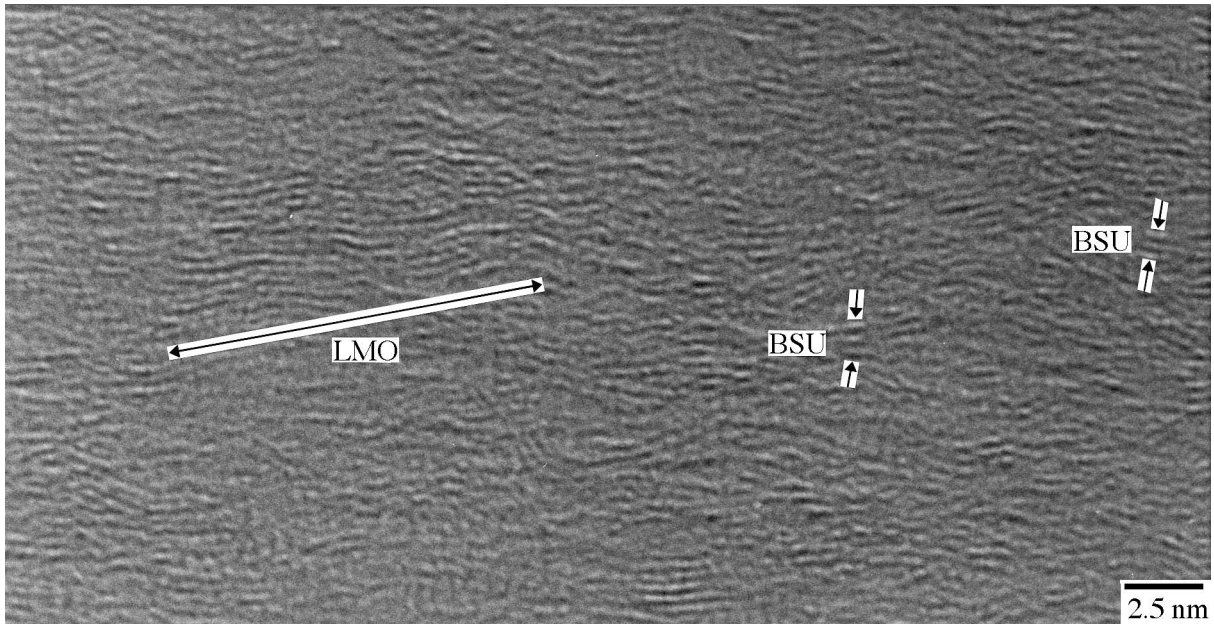

Fig. 3. HREM micrograph of a longitudinal section of the carbon fibre as in as-received 2·5D C_f–SiC composite.

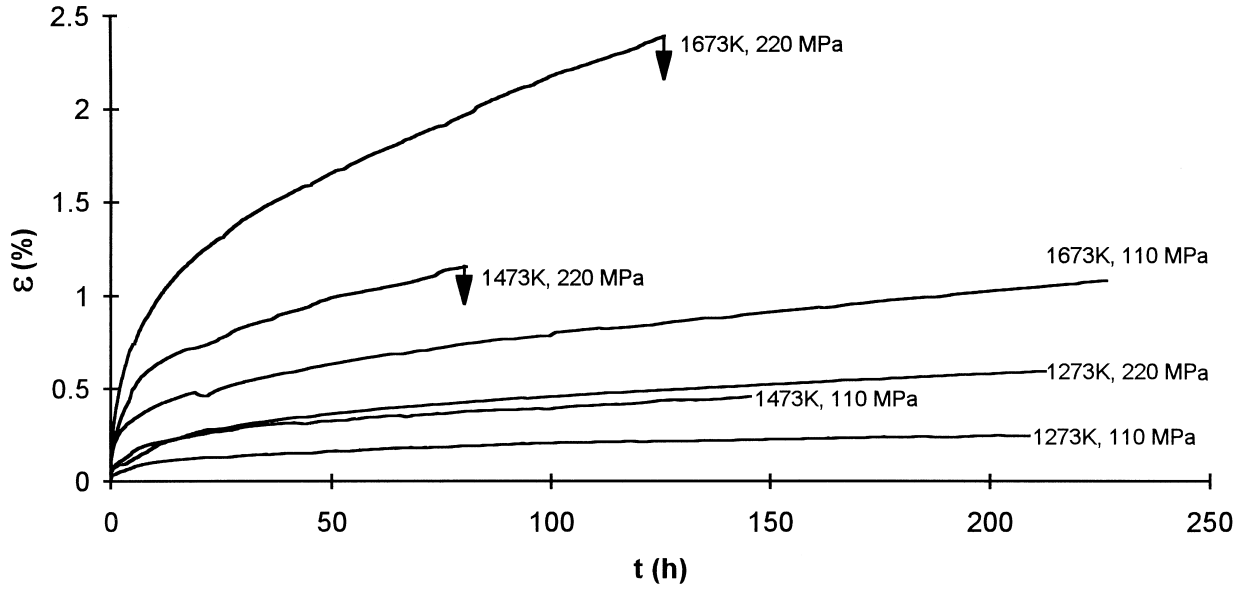

Fig. 4. Strain–time creep curves, $\varepsilon = f(t)$, for 2·5D C_f–SiC composites creep tested at different temperatures and stresses.

The occurrence of a transient creep stage followed by a steady-state has been demonstrated by plotting strain rates as a function of strain or time ($\dot{\varepsilon} = f(\varepsilon)$ or $\dot{\varepsilon} = f(t)$, (Fig. 5). The mean strain rates over these ranges of stresses and temperatures are between 2×10^{-9} s^{-1} (1273 K, 110 MPa) and 3×10^{-8} s^{-1} (1673 K, 220 MPa).

As for other CMCs with glass-ceramic or monolithic matrix, it has been shown that damage accumulation is responsible for creep strain in 2D SiC_f–MLAS[6,19] or in 2D $SiC_f - SiC$.[20] Moreover, in 2D C_f–SiC, Shuler *et al.*[21] have related the fatigue life at room-temperature to a microstructural damage dominated by the woven architecture of the composite. In the field of investigation considered here for 2·5D C_f–SiC composites, the same process seems very likely to occur. In a first approach of damage quantification, the damage function, D, was used as defined by Kachanov[22] as $D = 1 - (E_t/E_o)$, where E_t is the bulk elastic modulus of the composite at a time t and E_o the initial modulus of the composite right before

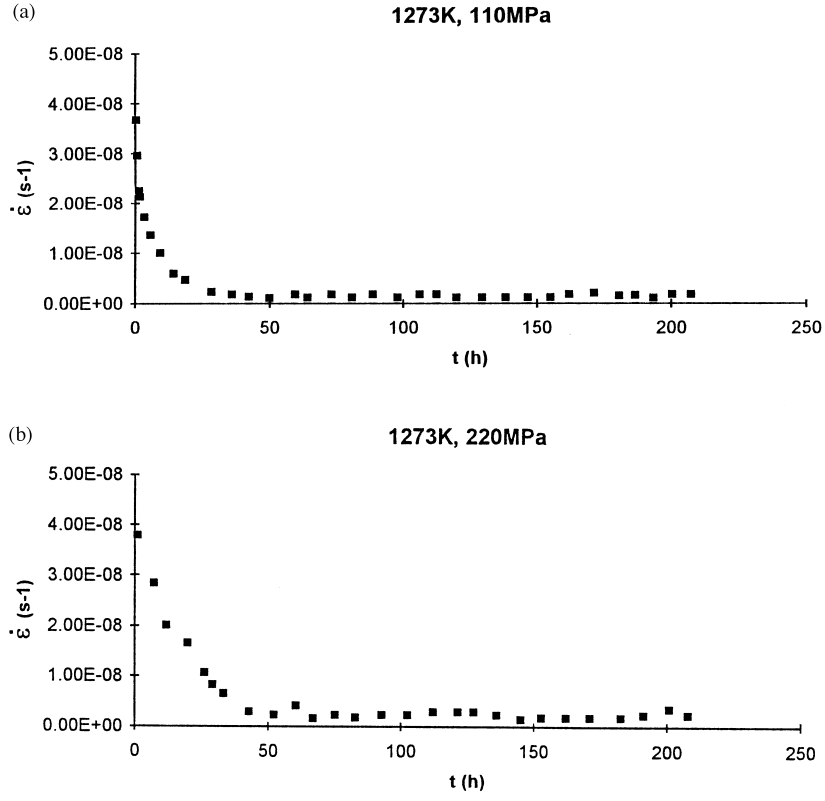

Fig. 5. Strain rates as a function of time, $\dot{\varepsilon} = f(t)$, for creep tests conducted at 1273 K under (a) 110 MPa and (b) 220 MPa.

creep starts. E_t was determined from unloading–reloading cycles during creep tests.

Study of the damage evolution (Fig. 6) reveals a damage–creep mechanism where damage accumulation seems to follow different regimes. For all temperatures, the main part of the damage is achieved in the transient creep stage due to time-dependent stress redistribution. At 1273 K, no significant damage evolution is observed in the steady-state compared to transient stage. At 1473 K, the damage evolution, D, follows several stages. Initially, the damage accumulation increases during the loading of the specimen and continues during the primary stage. However, the damage seems to decrease and returns the value obtained after loading. Finally, if the applied stress is 110 MPa, D will remain steady, but if the applied stress is 220 MPa, the damage increases again until rupture. The main difference between 1473 and 1673 K, concerns the duration of the stage where the damage remains steady.

To understand such a particular evolution and to assess the mechanisms responsible for creep a microstructural investigation at different scales is necessary.

4 Discussion

Part of the discussion of the macroscopic creep behaviour of the 2·5D C_f–SiC composite can be made through scanning and transmission electron

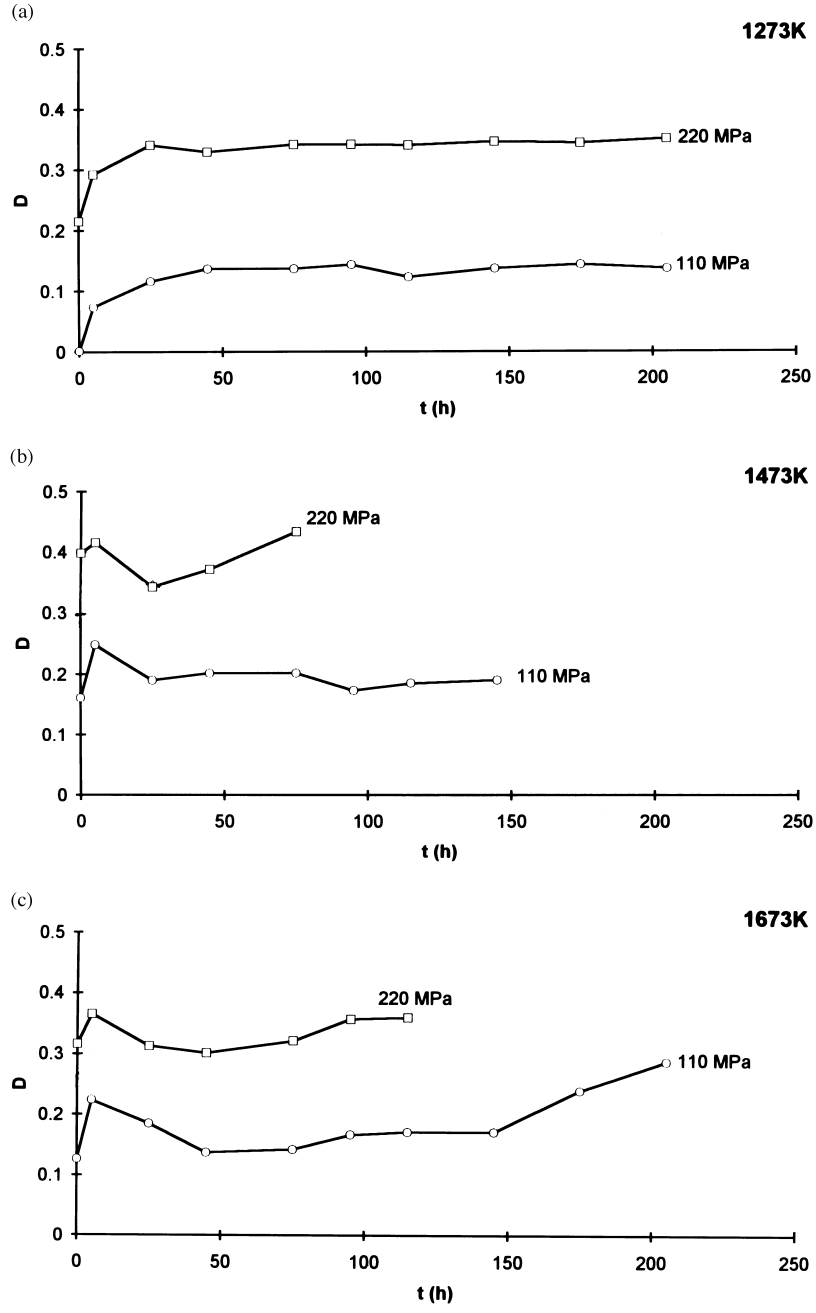

Fig. 6. Damage evolution upon creep tests conducted at (a) 1273, (b) 1473 and (c) 1673 K.

microscopy observations, which correspond to a microscopic-related macroscopic approach.

4.1 Damage observations

SEM investigations of the tested samples reveal that damage involves opening and coalescence of pre-existing cracks, and matrix microcracking at 110 MPa (Fig. 7), whereas such mechanisms are combined with formation of interply cracks parallel to the loading direction at 220 MPa (Fig. 8).

If we consider the surface of the samples (Figs 9 and 10), one can notice different types of cracks:

- transverse and longitudinal cracks in the transverse bundles,
- transverse and longitudinal cracks in the longitudinal bundles.

As a result, five different types of cracks have been identified:

1. transverse cracks in the transverse bundles,
2. transverse cracks in the longitudinal bundles,
3. longitudinal cracks in the longitudinal bundles,
4. longitudinal cracks in the transverse bundles,
5. interply cracks.

Types 1 and 3 cracks correspond to the pre-existing cracks. Type 2 cracks correspond to the transverse cracks generally observed in the unidirectional composites tested in tension.

From our observations in SEM,[1] it appears that the opening of the pre-existing cracks is the first damage mechanism observed followed by the formation of the transverse cracks in the longitudinal bundles (type 2) and also the initiation of interply cracks at the macropores. Then, as the opening of

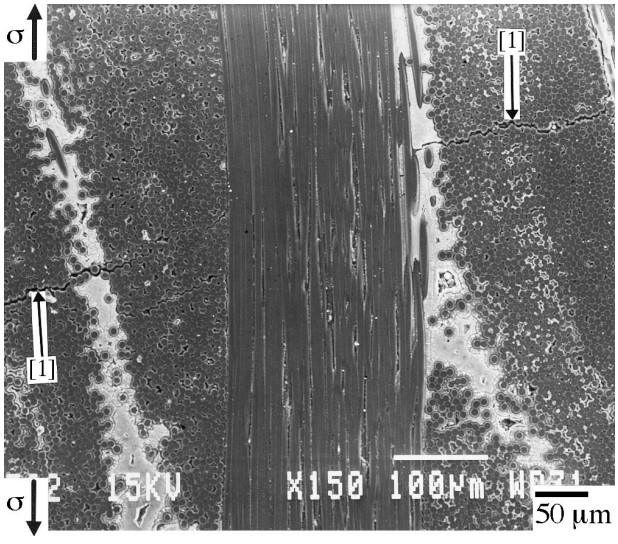

Fig. 7. SEM micrograph illustrating damage for a specimen creep tested at 1273 K under 110 MPa.

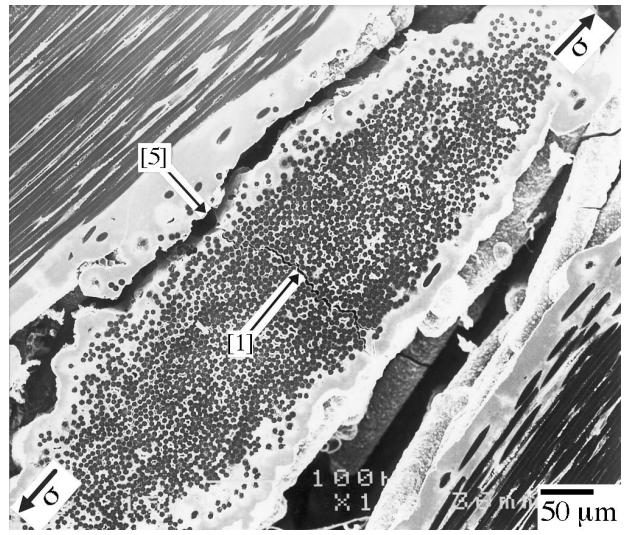

Fig. 8. SEM micrograph illustrating damage for a specimen creep tested at 1273 K under 220 MPa.

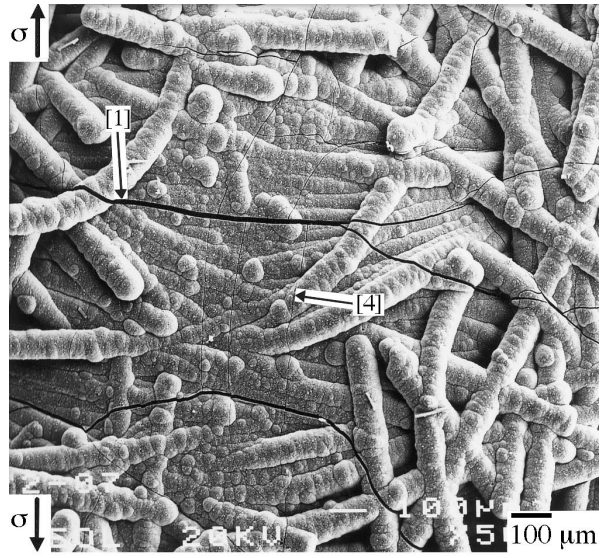

(a)

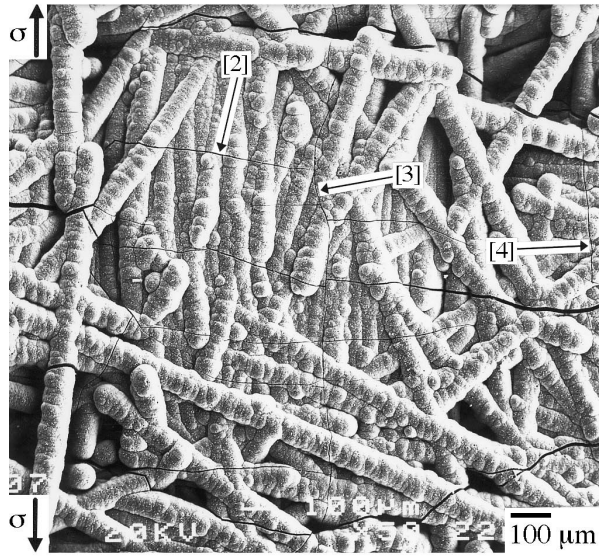

(b)

Fig. 9. SEM micrographs illustrating cracks at the surface of (a) a transverse and (b) a longitudinal bundle in a specimen creep tested at 1473 K under 220 MPa.

both types of transverse cracks continues, there is interconnection of the interply cracks with the creating of longitudinal cracks in the transverse bundles.

As a consequence of the different types of cracks observed, straightening of the longitudinal bundles parallel to the loading direction is admitted to be one of the driving forces for damage. As proposed by Shuler *et al.*,[21] such a straightening induces the initiation of interply microcracks (type 5) and the subsequent appearance of flexural forces in the transverse bundles leading to the opening of the pre-existing cracks (type 1) and the formation of type 4 cracks (Fig. 11).

Moreover, this microstructural investigation has revealed that crack opening is maintained upon unloading. From the macroscopic mechanical point of view, this can lead to an apparent stiffening of the composite,[23] which then leads to the damage reduction observed in Fig. 6(b) and (c).

These different conclusions can also be supported by morphological evolution determined quantitatively from automatic image analysis via mathematical morphology methods.[24]

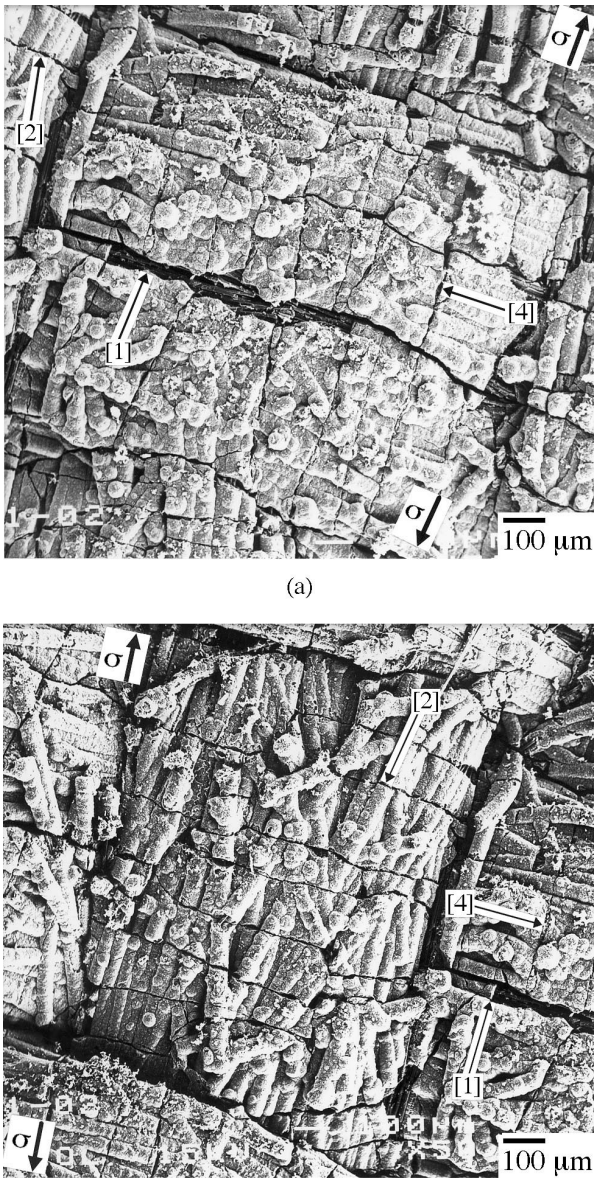

Fig. 10. SEM micrographs illustrating cracks at the surface of (a) a transverse and (b) a longitudinal bundle in a specimen creep tested at 1673 K under 220 MPa.

4.2 Nanoscale investigation of the constituents

In a recent work, we have investigated both the fibre and the matrix down to the nanometric scale via HREM.[1,25] At that scale, there is no evidence of structural changes in the matrix whereas only a slight effect on the texture of the fibre has been characterised with an increase of the local molecular orientations (LMOs) diameter up to 18 nm (1673 K, 220 MPa). Nevertheless, the resulting structure of the fibre is far from the texture of crept carbon fibres, but it can be considered as the first stage of the whole creep mechanism for carbon fibres. For this reason, the slight changes in the texture of the fibre at the nanometric scale has been called 'nanocreep' of the carbon fibre.[1,25]

In the meantime, observations of the fracture surfaces of the failed creep-tested specimens indicate two types of rupture coupled with various pull-out lengths and different surface roughness of the pyrocarbon interphase. Thus, the role of the pyrocarbon interphase is assumed to be of major importance. TEM and HREM investigations of the composite tested at 1673 K under 220 MPa, have shown a degradation of the interphase, located at the matrix/interphase interface as expected from its as-received texture.[15] The former highly anisotropic carbon layer tends to become distorted and amorphous (Fig. 12). The fibre/matrix sliding corresponds to a viscous-like flow which is consistent with the smooth pyrocarbon surface over the pull-out length on the fracture surface.

As a result, the contribution of the fibre to the macroscopic creep strain is considered as negligible compared to interfacial sliding and damage accumulation via matrix microcracking. Then, the first main damage appearance is due to matrix microcracking, whatever the temperature is. Different types of cracks are involved depending on whether

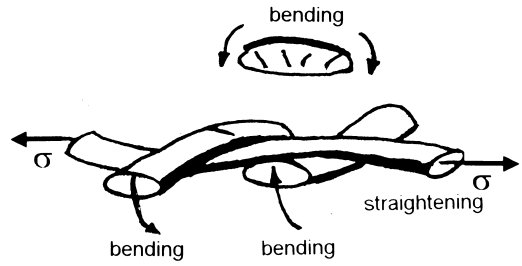

Fig. 11. Cracks generated by bending of the transverse bundles induced by straightening of the longitudinal bundles (after Shuler *et al.*[21]).

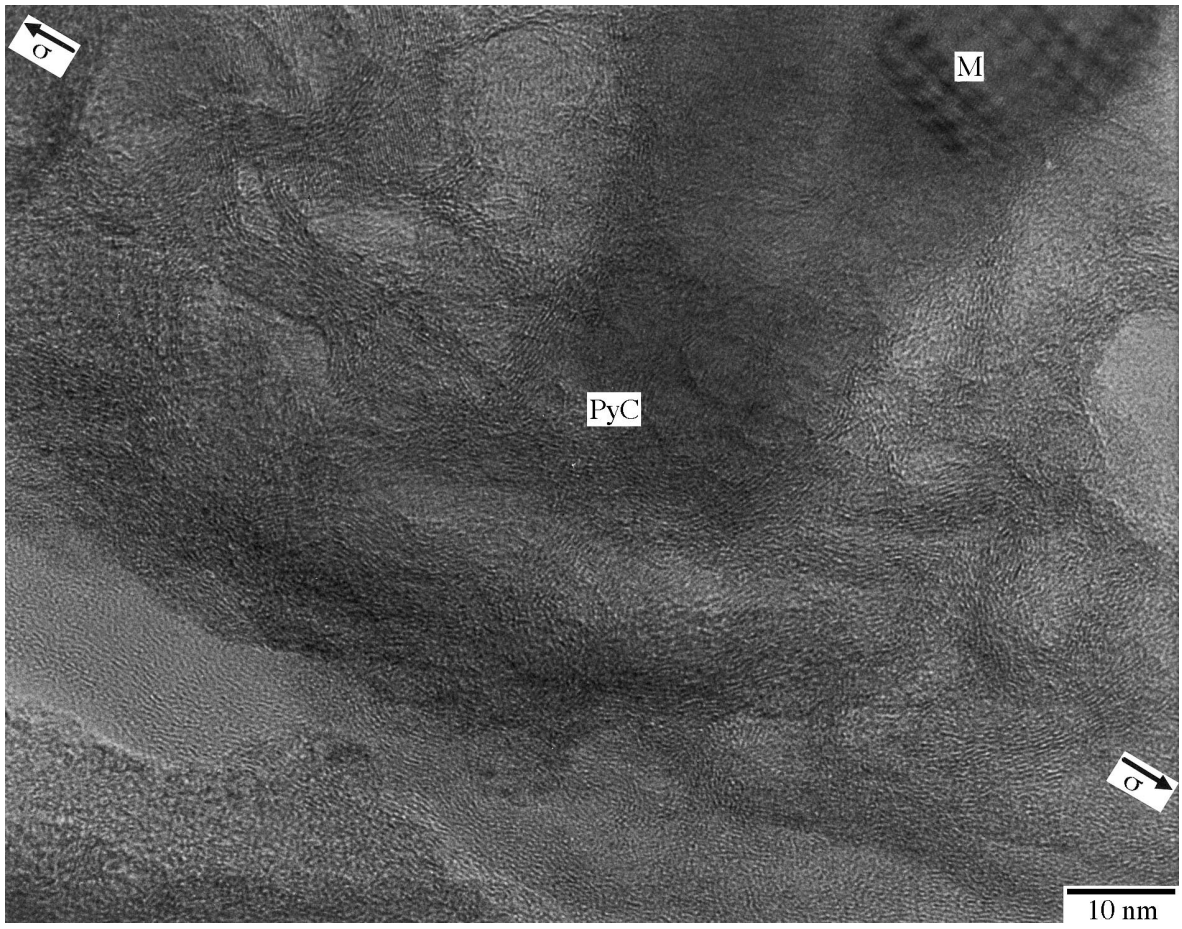

Fig. 12. HREM micrograph of the interphase/matrix interface in a 2·5D C_f–SiC composite creep tested at 1673 K under 220 MPa.

the stress is high or low. As already shown by Shuler *et al.*,[21] straightening of the longitudinal bundles parallel to the loading axis is the driving force for matrix microcracking as it initiates interply microcracks at the macropores and subsequent longitudinal cracks in the transverse bundles. The difference in time and strain to failure observed between 1473 and 1673 K can be attributed to a time-dependent mechanism governed by two different types of sliding at the fibre/matrix interface:[1] a viscous-like flow at 1673 K and a dry friction-like behaviour between rough solids at 1473 K.

5 Conclusion

C_f–SiC composites have shown a good creep resistance upon tests between 1273 and 1673 K under 110 and 220 MPa. The occurrence of a steady-state creep has been evidenced for both stress levels. Creep rates in the 10^{-9}–10^{-8} s^{-1} range have been obtained.

In that experimental domain, the macroscopic results, coupled with microscopic observations at different scales confirm a damage-creep mechanism, as also observed in CMCs with glass-ceramic matrices.[5–8] Some of the damage mechanisms have already been identified such as five types of matrix microcracking, but further investigations are necessary.

The nanostructural characterisation of the phases via HREM can stand as a reference to determine their evolution. A special care has been focused on the changes in BSUs and LMOs sizes.

The role of the interphase and the fibre/matrix sliding appear to be of major importance regarding macroscopic creep strain in the investigated stress and temperature domains, whereas the role of the fibre, from the macroscopic creep strain point of view, appears to be negligible.

Acknowledgements

This work has been performed with the support (G.B.) of the SEP, Division de SNECMA, St-Médard en Jalles, France, and Région de Basse-Normandie. We want to thank particularly Drs J. P. Richard and F. Abbé for fruitful discussions.

References

1. Boitier, G., Comportement en fluage et microstructure de composites C_f–SiC 2·5D. Thése de Doctorat, University of Caen, France, 1997.

2. Dalmaz, A., Etude du comportement en fatigue cyclique du composite tissé fibre de carbone/matrice carbure de silicium 2·5D C/SiC. Thése de Doctorat, INSA of Lyon, France, 1997.
3. Brennan, J. J., Interfacial characterization of glass and glass–ceramic matrix/Nicalon SiC fiber composites. In *Tailoring Multiphase and Composite Ceramics*, ed. R. E. Tressler, G. L. Messing, C. G. Pantano and R. E. Newham. Materials Science Research, Plenum Press, New York, 1986, pp. 549–560.
4. Kerans, R. J., Hay, R. S., Pagano, N. J. and Parthasarthy, T. A., The role of fiber-matrix interface in ceramic composites. *Amer. Ceram. Soc. Bul.*, 1989, **68**, 429–442.
5. Kervadec, D., Comportement en fluage sous flexion et microstructure d'un SiC_f–MLAS 1D. Thése de Doctorat, the University of Caen, France, 1992.
6. Maupas, H., Fluage d'un composite SiC_f–MLAS 2D en flexion et en traction. Thése de Doctorat, the University of Caen, France, 1996.
7. Vicens, J., Doreau, F. and Chermant, J. L., Microstructural characterization of SiC_f/YMAS composites in the as-received state and after thermomechanical tests. *Composites: Part A*, 1996, **27A**, 723–727.
8. Chermant, J. L., Creep behaviour of ceramic matrix composites. *Sil. Ind.*, 1995, **60**, 261–273.
9. Luecke, W. E. and Wiederhorn, S. M., Interlaboratory verification of silicon nitride creep properties. *J. Amer. Ceram. Soc.*, 1997, **80**, 831–838.
10. Boitier, G., Maupas, H., Cubéro, H. and Chermant, J. L., Sur les essais de traction à longs termes à haute température. *Rev. Comp. Mat. Avancés*, 1997, **7**, 143–172.
11. Boitier, G., Cubéro, H. and Chermant, J. L., Some recommendations for long term high temperature tests. In: *3rd International Conference on High Temperature Ceramic Matrix Composites, HT-CMC3*, ed. K. K. Niihara and K. Nakano, 6–9 September 1988, Osaka, Japan.
12. Boitier, G., Vicens, J. and Chermant, J. L., Nanostructure study by TEM and HREM of carbon fibres in C_f–SiC composites. *J. Mat. Sci. Lett*, 1977, **16**, 1402–1405.
13. Boitier, G., Vicens, J. and Chermant, J. L., Microstructure of C_f–SiC composites. In *Ceramic and Metal Matrix Composites, CMMC 96*, Vols 127–131, ed. M. Fuentes, J. M. Martinez-Esnaola and A. M. Daniel. Key Eng. Mat. Trans Technical, Vetikom-Zurich, CH, pp. 777–784.
14. Christin, F., Les composites carbone-carbure de silicium: une nouvelle famille de matériaux destinés à des applications à haute température. Thése de Doctorat ès Sciences, University of Bordeaux I, France, 1979.
15. Després, J. F. and Monthioux, M., Mechanical properties of C/SiC composites as explained from their interfacial features. *Journal of the European Ceramic Society*, 1995, **15**, 209–224.
16. Guigon, M., Oberlin, A. and Desarmot, G., Microtexture and structure of some high tensile strength PAN based carbon fibres. *Fib. Sci. Tech.*, 1984, **20**, 55–72.
17. Dalmaz, A., Reynaud, P., Rouby, D. and Fantozzi, G., Damage propagation in carbon/silicon carbide composites during tensile tests under the SEM. *J. Mat. Sci.*, 1996, **31**, 4213–4219.
18. Lorrain, B. and Lachaud, F., Endommagement dynamique des matériaux carbone–SiC: influence du chargement sur la rupture. In *Comptes Rendus des 10émes Journées Nationales sur les Composites, JNC 10*, ed. D. Baptiste and A. Vautrin, ENSAM, Paris France, AMAC, Paris, 29–31 October 1996, pp. 1249–1258.
19. Maupas, H., Kervadec, D. and Chermant, J. L., Damage creep in SiC_f–MLAS composites. In *Fracture Mechanics of Ceramics—Fatigue, Composites and High Temperature Behaviour*, Vol 12, ed. R. C. Brandt, D. P. H. Hasselman, D. Munz, M. Sakai and V. Ya. Shevchenko. Plenum Press, New York, 1996, pp. 527–538.
20. Abbé, F., Fluage en flexion d'un composite SiC_f–SiC 2D. Thése de Doctorat, the University of Caen, 1990.
21. Shuler, S. F., Holmes, J. W., Wu, X. and Roach, D., Influence of loading frequency on the room-temperature fatigue of a carbon-fiber/SiC-matrix composite. *J. Amer. Ceram. Soc.*, 1993, **76**, 2327–2336.
22. Kachanov, L., Rupture time under creep conditions. *Izv. Akad. Nauk. SSR*, 1958, **8**, 26–31.
23. Reynaud, P., Dalmaz, A., Rouby, D. and Fantozzi, G., Mechanical stiffening of ceramic matrix composites induced by cyclic fatigue. *Key Eng. Mat.*, 1997, **132–136**, pp. 1906–1909.
24. Boitier, G., Chermant, L. and Chermant, J. L., Morphological quantification of carbon–silicon carbide composites. *Acta Stereol*, 1998, **17**, 275–280.
25. Boitier, G., Vicens, J. and Chermant, J. L., Carbon fiber "nanocreep" in creep-tested C_f–SiC composites. *Script. Mat.*, 1998, **38**, 937–943.